Supplementary Materials

Dimetal and duplex heteroatoms co-doped graphene aerogel in electrolytic CO_2 reduction to CO in aqueous electrolyte

Hui-Hui Cao[1], Zhen-Hong He[1,*], Pan-Pan Guo[1], Yue Tian[1], Xin Wang[1], Kuan Wang[1], Weitao Wang[1], Huan Wang[1], Zhao-Tie Liu[1,2,*]

[1]Shaanxi Key Laboratory of Chemical Additives for Industry, College of Chemistry and Chemical Engineering, Shaanxi University of Science & Technology, Xi'an 710021, Shaanxi, China.
[2]School of Chemistry & Chemical Engineering, Shaanxi Normal University, Xi'an 710119, Shaanxi, China.

[*]**Correspondence to:** Prof. Zhen-Hong He, Shaanxi Key Laboratory of Chemical Additives for Industry, College of Chemistry and Chemical Engineering, Shaanxi University of Science & Technology, Xi'an 710021, Shaanxi, China. E-mail: hezhenhong@sust.edu.cn; Prof. Zhao-Tie Liu, School of Chemistry & Chemical Engineering, Shaanxi Normal University, Xi'an 710119, Shaanxi, China. E-mail: ztliu@snnu.edu.cn

Supplementary Table 1. Electrocatalytic reduction of CO_2 to CO over diverse reported catalysts

Number	Catalysts	E (V, *vs*. RHE)	*j* (mA/cm^2)	FE_{CO} (%)	Stability (h)	Res.
1	[Mn-2,6-bis(1-(alkyl)imidazol-2-ylidene)pyridine]Br pincer complex	-	-	86 ± 4	-	[1]
2	[Mn-MeCN]/MWCNT	-0.39	-2.6 ~-2.0	84±4	24	[2]
3	fac-$Mn(CO)_3$ bipyridine complex	-1.56	About 1.3	77.7	-	[3]
4	CMP-$(bpy)_{20}$-Mn	-1.60	−0.01	0.43	3	[4]
5	fac-Mn(apbpy)$(CO)_3$Br complex	-1.35	About 14.0	60	10	[5]
6	[Mn$(bpy(R)_2)(CO)_3$Br] /nc-TiO_2	-0.30	-	60	-	[6]
7	URA-Mn2	-1.20	-	60	4	[7]
8	MnBr(6-(2-hydroxyphenol)-2,2′-bipyridine)$(CO)_3$	-0.44	3.1	76	4	[8]
9	MnO/NGA	-0.82	About −10	86	10	[9]
10	Mn(bpy-tBu)$(CO)_3$Br	-2.2 (V, *vs*. SCE)	-	100 ± 15	-	[10]
11	[MnBr(2,2′-bipyridine)$(CO)_3$] complex	-1.1	About −17	About 35	-	[11]
12	Fe–N–C	-0.09	17.5	93.5	-	[12]
13	$Zn_{1.5}Mg_{1.5}Al_1$-LDH	-1.40	5.9	91.8	9	[13]
14	ZnO/Zn foils	-2.00	11.5	85.0	-	[14]
15	Cu_{25}Zn-A	-0.98	9.2	94.0	11	[15]
16	Cu-In/PNGC	-0.59	136.4	91.3	5	[16]
17	$CuZn_x$/NGN	-0.8	3.9	<50	24	[17]
18	MnZn/N,P-3D-GA	-0.92	12.0	96.6	20	This work

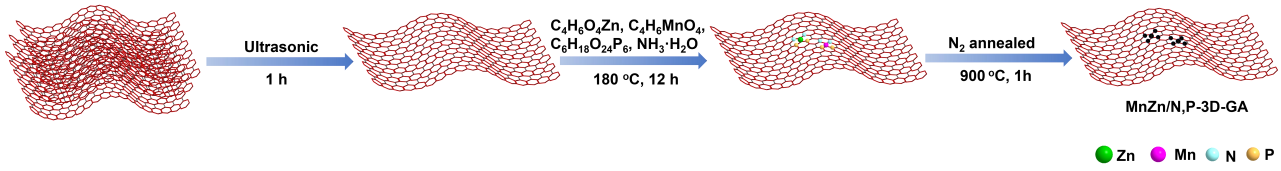

Supplementary Scheme 1. Synthesis procedures of the MnZn/N,P-3D-GA catalyst.

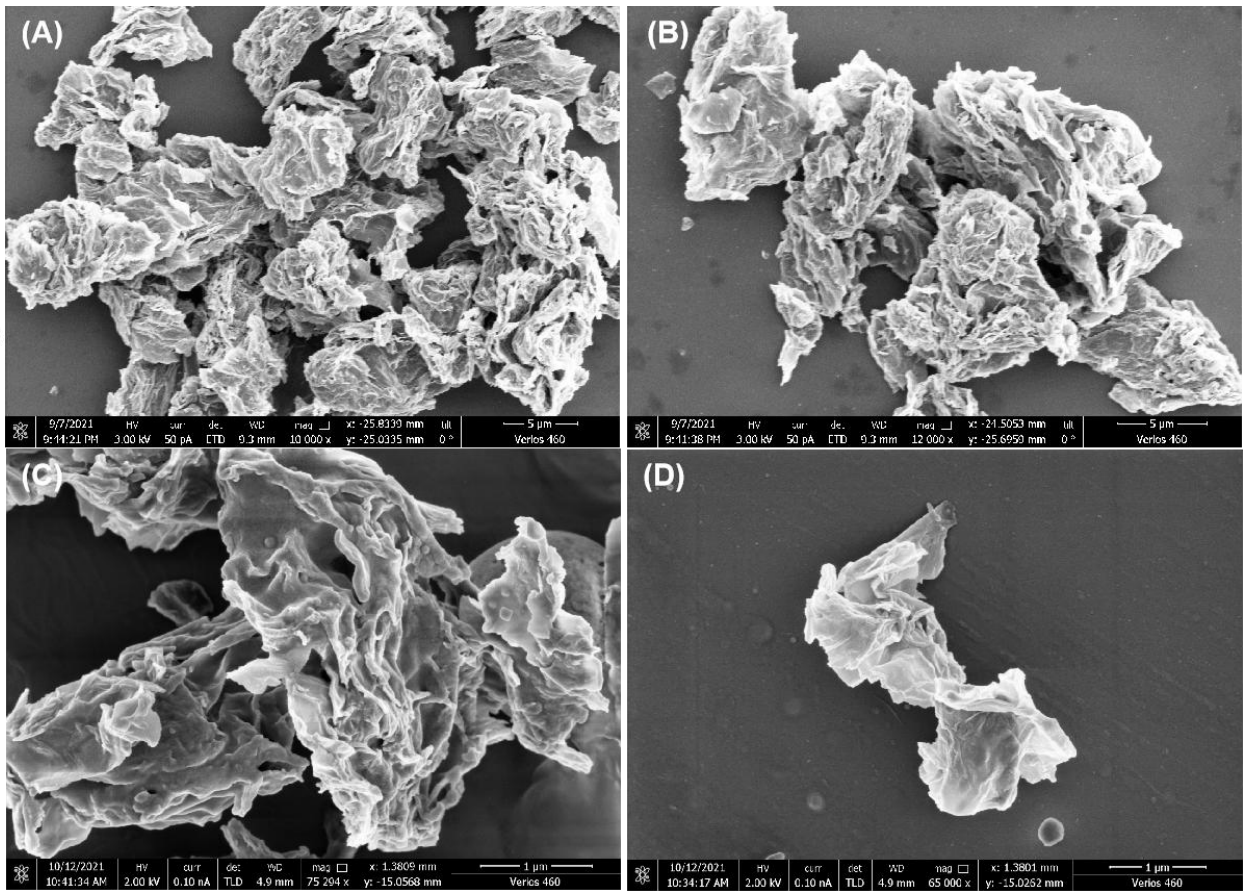

Supplementary Figure 1. SEM images of the MnZn/N,P-3D-GA catalyst.

Supplementary Table 2. The analysis results of N_2 adsorption/desorption isotherms for catalysts

Catalysts	BET surface area (m^2/g)	Pore size (nm)	Pore volume (cm^3/g)
GA	311	10.9	0.84
N,P-3D-GA	205	13.2	0.68
Zn/N,P-3D-GA	225	12.6	0.70
Mn/N,P-3D-GA	158	13.1	0.52
MnZn/N,P-3D-GA	241	11.9	0.71

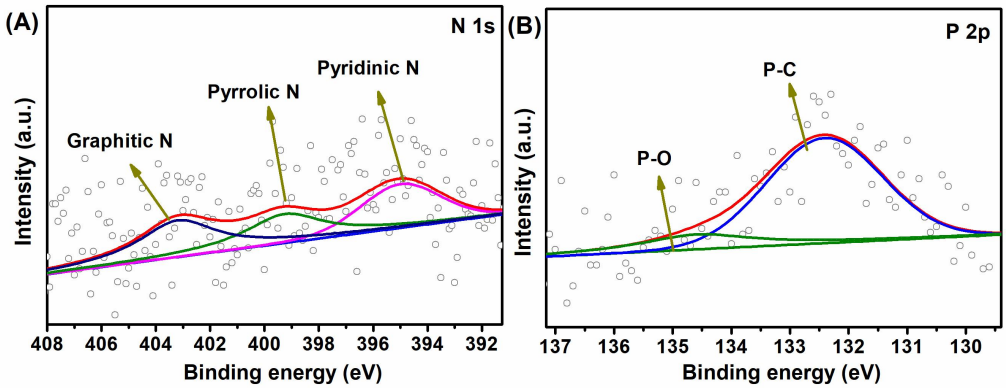

Supplementary Figure 2. XPS spectra of N,P-3D-GA, including N 1s spectrum (A) and P 2p spectrum (B).

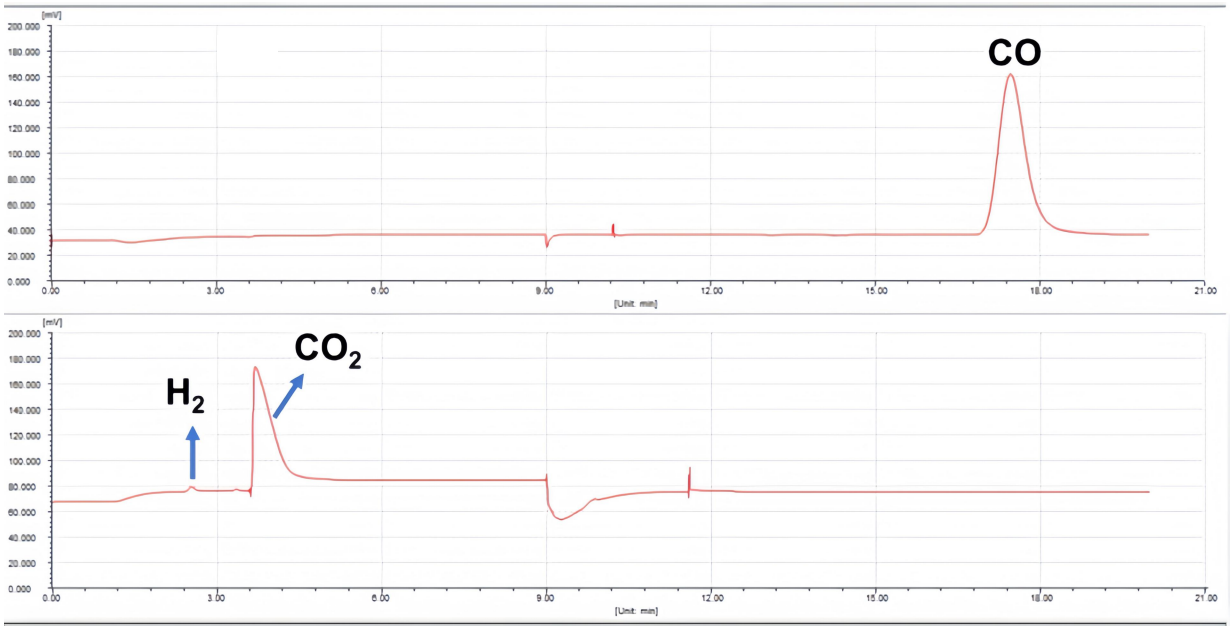

Supplementary Figure 3. GC results of CO_2ER over the MnZn/N,P-3D-GA catalyst.

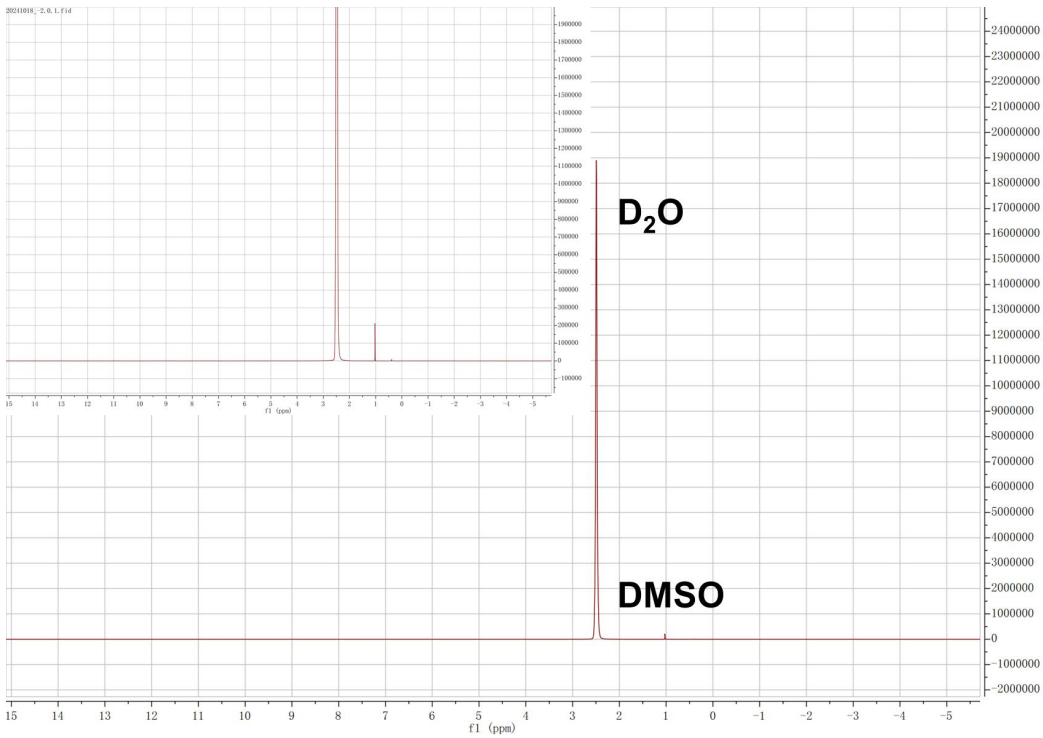

Supplementary Figure 4. Representative ^{1}H NMR spectrum. The ^{1}H NMR spectrum of the liquid products was obtained upon CO_2ER on MnZn/N,P-3D-GA electrode at -0.92 V (*vs.* RHE) for 30 min. DMSO was used as an internal standard for quantification of liquid products.

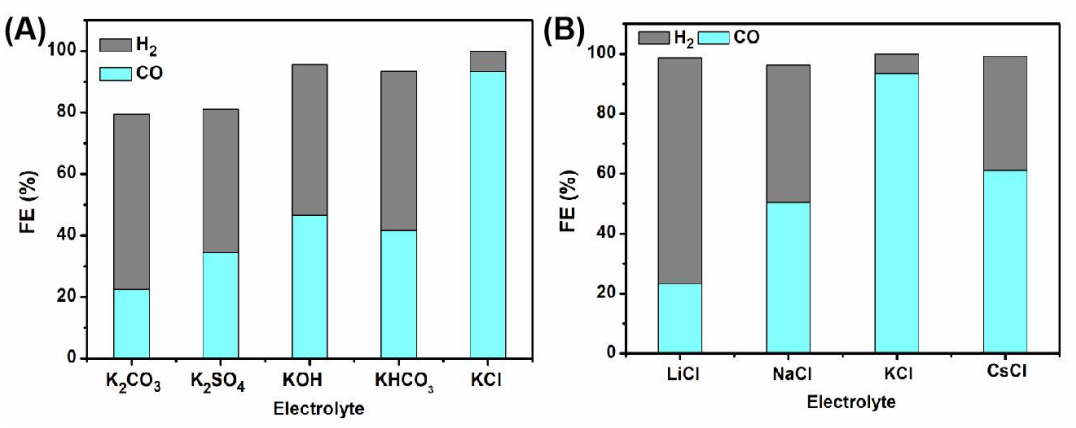

Supplementary Figure 5. FE_{H2} and FE_{CO} over the MnZn/N,P-3D-GA catalyst in different anion electrolytes containing 0.1 M K^+ (A) and FE_{H2} and FE_{CO} over the MnZn/N,P-3D-GA catalyst in different alkali metal electrolytes containing 0.1 M Cl^- (B).

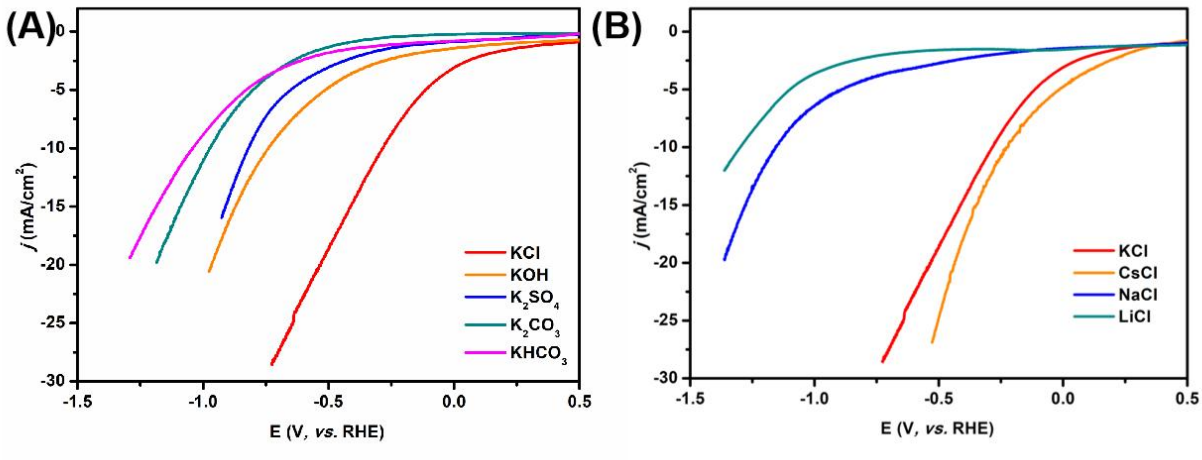

Supplementary Figure 6. LSV curves over the MnZn/N,P-3D-GA catalyst in different anion electrolytes containing 0.1 M K^+ (A) and LSV curves over the MnZn/N,P-3D-GA catalyst in different alkali metal electrolytes containing 0.1 M Cl^- (B).

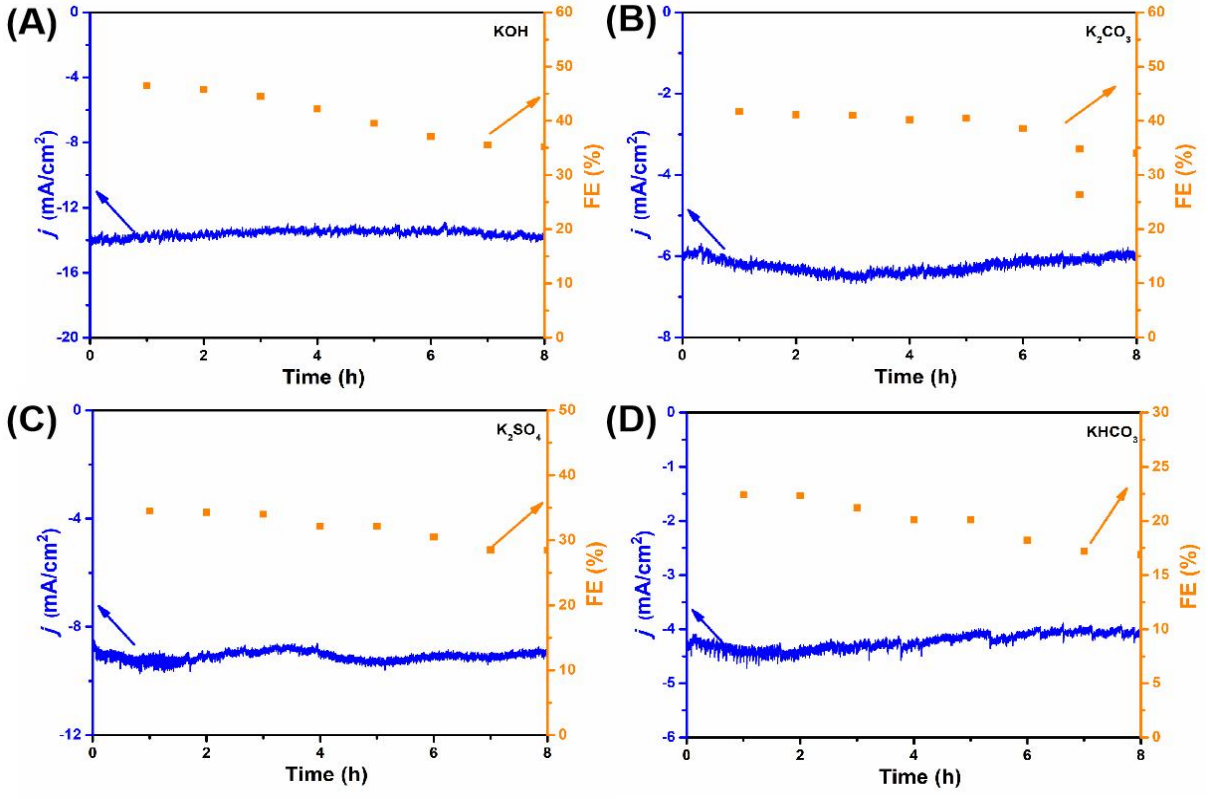

Supplementary Figure 7. The stability of MnZn/N,P-3D-GA at -0.92 V (*vs*. RHE) in a CO_2-saturated 0.1 M KOH (A), 0.05 M K_2CO_3 (B), 0.05 M K_2SO_4 (C), and 0.1 M $KHCO_3$ (D) electrolyte.

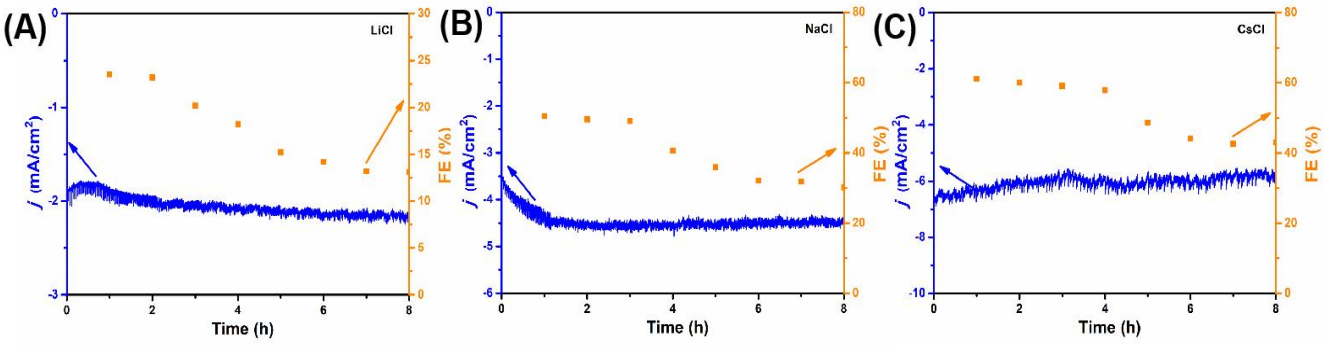

Supplementary Figure 8. The stability of MnZn/N,P-3D-GA at -0.92 V (*vs*. RHE) in a CO_2-saturated 0.1 M LiCl (A), 0.1 M NaCl (B), and 0.1 M CsCl (C) electrolyte.

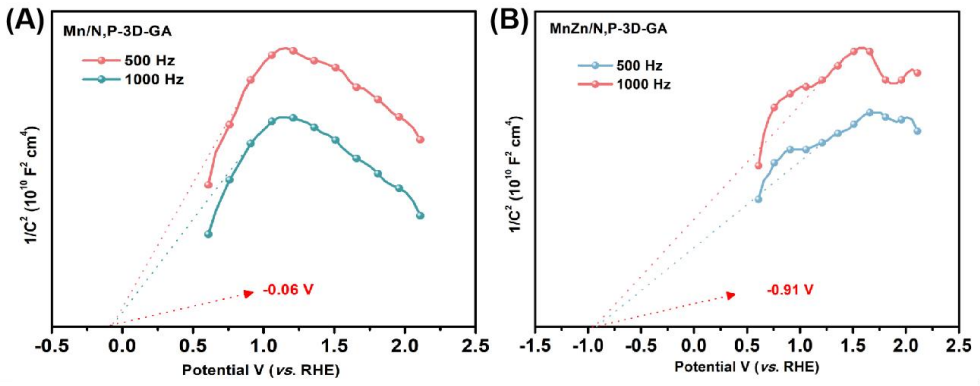

Supplementary Figure 9. Mott-Schottky curves of Mn/N,P-3D-GA (A) and MnZn/N,P-3D-GA (B).

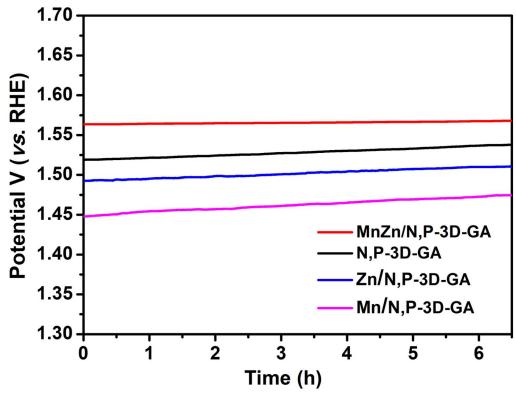

Supplementary Figure 10. The open circuit voltages of MnZn/N,P-3D-GA, N,P-3D-GA, Zn/N,P-3D-GA and Mn/N,P-3D-GA.

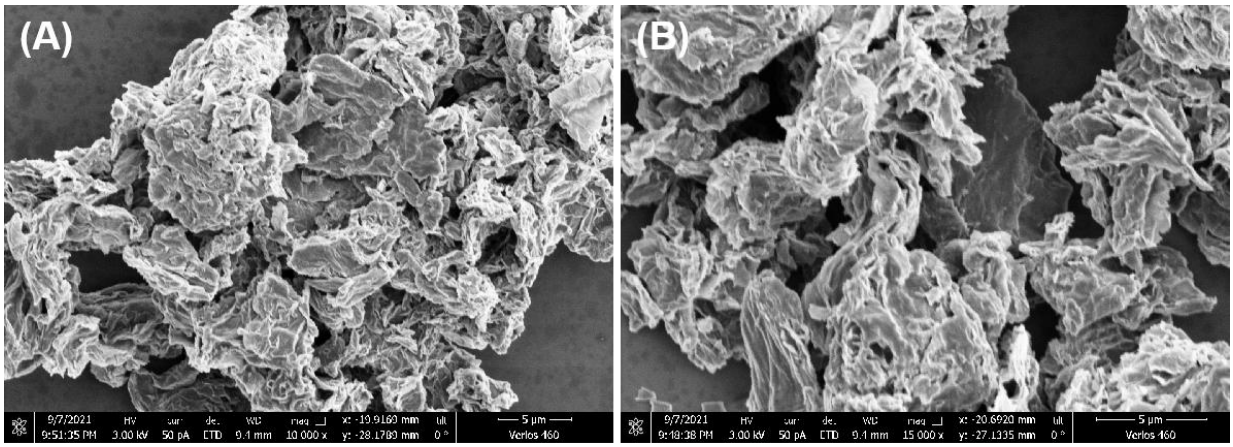

Supplementary Figure 11. SEM images of the used MnZn/N,P-3D-GA catalyst.

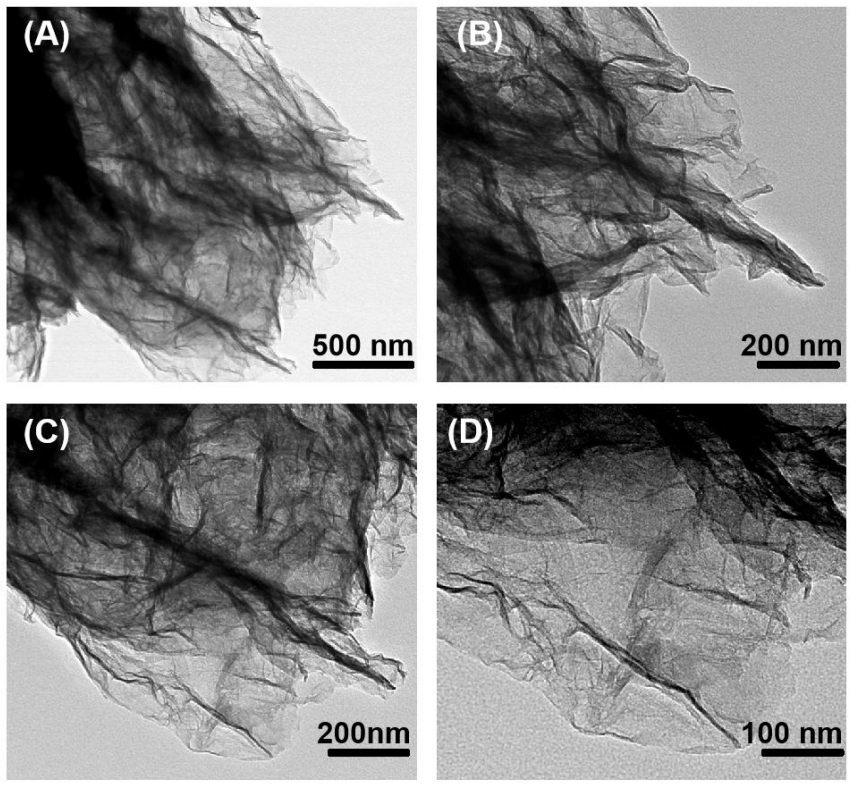

Supplementary Figure 12. TEM images of the used MnZn/N,P-3D-GA catalyst.

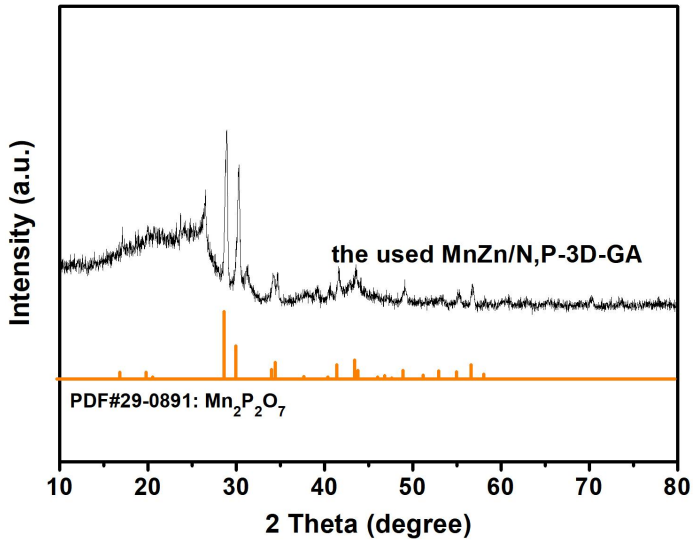

Supplementary Figure 13. XRD of the used MnZn/N,P-3D-GA catalyst.

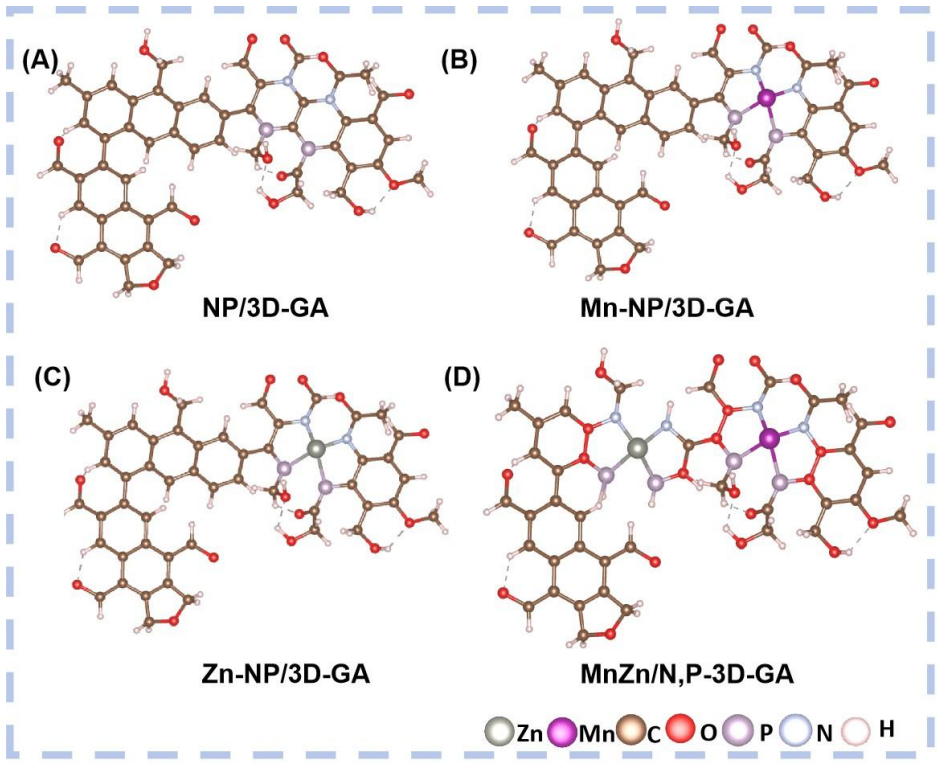

Supplementary Figure 14. Optimized catalyst structures.

References

[1] Myren TH, Alherz A, Thurston JR, et al. Mn-based Molecular catalysts for the electrocatalytic disproportionation of CO_2 into CO and CO_3^{2-}. *ACS Catal* 2020; 10: 1961-1968. https://doi.org/10.1021/acscatal.9b04773

[2] Sato S., Saita K., Sekizawa K., Maeda S., Morikawa T. Low-energy electrocatalytic CO_2 reduction in water over Mn-complex catalyst electrode aided by a nanocarbon support and K^+ cations. *ACS Catal* 2018; 8: 4452-4458. https://doi.org/10.1021/acscatal.8b01068

[3] Sung S, Li X, Wolf LM, et al. Synergistic effects of imidazolium-functionalization on fac-$Mn(CO)_3$ bipyridine catalyst platforms for electrocatalytic carbon dioxide reduction. *J Am Chem Soc* 2019; 141: 6569-6582. https://doi.org/10.1021/jacs.8b13657

[4] Smith C.L., Clowes R., Sprick R.S., Cooper A.I., Cowan A.J. Metal-organic conjugated microporous polymer containing a carbon dioxide reduction electrocatalyst. *Sustain Energ Fuels* 2019; 3: 2990-2994. https://doi.org/10.1039/C9SE00450E

[5] Rotundo L, Filippi J, Gobetto R, et al. Electrochemical CO_2 reduction in water at carbon cloth electrodes functionalized with a fac-Mn(apbpy)$(CO)_3$Br complex. *Chem Comm* 2019; 55: 775-777. https://doi.org/10.1039/C8CC08385A

[6] Walsh J.J., Forster M., Smith C.L., Neri G., Potter R.J., Cowan A.J. Directing the mechanism of CO_2 reduction by a Mn catalyst through surface immobilization. *Phys Chem Chem Phys* 2018; 20: 6811-6816. https://doi.org/10.1039/C7CP08537K

[7] Kossmann J., Sánchez-Manjavacas M.L., Brandt J., Heil T., López-Salas N., Albero J. Mn(ii) sub-nanometric site stabilization in noble, N-doped carbonaceous materials for electrochemical CO_2 reduction. *Chem Comm* 2022; 58: 4841-4844. https://doi.org/10.1021/acs.inorgchem.5b00233

[8] Agarwal J., Shaw T.W., Schaefer H.F., Bocarsly A.B. Design of a catalytic active site for electrochemical CO_2 reduction with Mn(I)-tricarbonyl species. *Inorg Chem* 2015; 54: 5285-5294. https://doi.org/10.1021/acs.inorgchem.5b00233

[9] Wang M, Zhang B, Ding J, et al. Three-dimensional nitrogen-doped graphene aerogel-supported MnO nanoparticles as efficient electrocatalysts for CO_2 reduction to CO. *ACS Sustain Chem Eng* 2020; 8: 4983-4994. https://doi.org/10.1021/acssuschemeng.0c01194

[10] Smieja J.M., Sampson M.D., Grice K.A., Benson E.E., Froehlich J.D., Kubiak C.P. Manganese as a substitute for rhenium in CO_2 reduction catalysts: the importance of acids. *Inorg Chem Front* 2013; 52: 2484-91. https://doi.org/10.1021/ic302391u

[11] Reuillard B., Ly K.H., Rosser T.E., Kuehnel M.F., Zebger I., Reisner E. Tuning product selectivity for aqueous CO_2 reduction with a Mn(bipyridine)-pyrene catalyst immobilized on a carbon nanotube electrode. *J Am Chem Soc* 2017; 139: 14425-14435. https://doi.org/10.1021/jacs.7b06269

[12] Zhang C, Yang S, Wu J, et al. Electrochemical CO_2 reduction with atomic iron-dispersed on nitrogen-doped graphene. *Adv Energy Mater* 2018; 8: 101382. https://doi.org/10.1002/aenm.201703487

[13] Ma X., Liu T., Lu B., Zhang Y. Synergistic effect of ZnMgAl-hydrotalcite nanomaterials electrocatalysts on high efficiency electrocatalytic reduction of CO_2 to CO. *J Alloy Compd* 2024; 973:172858. https://doi.org/10.1016/j.jallcom.2023.172858

[14] Xiang Q, Li F, Wang J, et al. Heterostructure of ZnO nanosheets/Zn with a highly enhanced edge surface forefficient CO_2 electrochemical reduction to CO. *ACS Appl Mater Inter* 2021; 13: 10837-10844. https://doi.org/10.1021/acsami.0c20302

[15] Feng J, Li J, Qiao L, et al. Reconstructed anti-poisoning surface for enhanced electrochemical CO_2 reduction on Cu-incorporated ZnO. *Appl Catal B-Environ* 2023; 330: 0926-3373. https://doi.org/10.1016/j.apcatb.2023.122665

[16] Zhang X, Zhu Y, Liu Z, et al. Perforated nitrogen-rich graphene-like carbon nanolayers supported Cu-In catalyst for boosting CO_2 electroreduction to CO. *J Energy Chem* 2022; 75: 383-390. https://doi.org/10.1016/j.jechem.2022.09.003

[17] Dongare S., Singh N., Bhunia H. Oxide-derived Cu-Zn nanoparticles supported on N-doped graphene for electrochemical reduction of CO_2 to ethanol. *Appl Surf Sci* 2021; 556: 149790. https://doi.org/10.1016/j.apsusc.2021.149790